O.Scherf, B.Simeon

Viscoplastic Deformation from the DAE Perspective - a Benchmark Problem

Viscoplastic deformation is characterized by a combined system of balance and evolution equations. The application of the Finite Element Method results in a Differential-Algebraic Equation (DAE) in time. The paper summarizes the most important points of the mathematical model and presents a benchmark problem for numerical comparisons. As computational example, the BDF-2 method with stepsize control is applied.

1. Introduction

Deformation and failure of technical structures are a focus of current research in computational mechanics. Simulation techniques in this field rely mainly on the Finite Element Method (FEM) and corresponding numerical software [4]. For time dependent material laws, not only the space but also the time dimension plays an important role. In particular in viscoplasticity, there is a growing interest in the DAEs that arise after space discretization. The goal is the combination of numerical techniques from FEM and DAEs in order to achieve more accurate results and better performance. Since it is often very difficult to assess the quality of a method, there is a need for benchmark problems which show typical difficulties but can still be handled outside a black box simulation environment.

In this paper, we concentrate on the time dimension and discuss viscoplastic deformation from the DAE perspective. Moreover, we present a test problem which is intended to serve as a reference for numerical methods. Section 2 specifies the combined system of balance equations for the displacements and evolution equations for the internal variables. In Section 3, the space discretization and the resulting DAE in time are introduced. Furthermore, the index is determined and the potential of stiff DAE solvers is investigated. Finally, the example of a viscoplastic beam subjected to a tensile and a bending test illustrates the problem class. The DAE is solved by both implicit Euler and the BDF-2 method with stepsize control. We give all the data necessary for 2D simulation and provide in this way a benchmark problem for further comparisons.

2. Mathematical Model

We consider a body $\Omega \subset \mathbb{R}^3$ with sufficiently smooth boundary $\partial\Omega$. Cauchy's first law of motion characterizes the deformed body by

$$\rho(x,t)\,\ddot{u}(x,t) = div\,\boldsymbol{\sigma}(x,t) + f(x,t) \qquad \forall x \in \Omega \tag{1}$$

with boundary conditions $u(x,t) = \bar{u}(x,t)\ \forall x \in \partial\Omega_u$ and $\boldsymbol{\sigma}(x,t)\,n(x,t) = \bar{t}(x,t)\ \forall x \in \partial\Omega_\sigma$. Here, u stands for the displacements, $\boldsymbol{\sigma}$ is the symmetric stress tensor, ρ the mass density and f the density of body forces. Furthermore, $\bar{u}$ denotes prescribed displacements, $\bar{t}$ surface tractions, and n is the unit normal vector on $\partial\Omega_\sigma$ with $\partial\Omega = \partial\Omega_\sigma \cup \partial\Omega_u$.

As usual in viscoplasticity, we neglect the acceleration term $\ddot{u}$ in (1) because we are only interested in long term loads. A material law completes the equations of motion by relating stress and strain. The standard assumption in viscoplasticity is that the total strain tensor $\boldsymbol{\varepsilon}$ can be decomposed additively into an elastic part $\boldsymbol{\varepsilon}^e$ and a plastic part $\boldsymbol{\varepsilon}^p$ [12]. We restrict the discussion to the geometrically linear case and Hooke's law for the elastic part whence

$$\varepsilon(x,t) = \frac{1}{2}(\nabla u(x,t) + (\nabla u(x,t))^T), \qquad \boldsymbol{\sigma}(x,t) = \boldsymbol{D}\boldsymbol{\varepsilon}^e(x,t) = \boldsymbol{D}(\varepsilon(x,t) - \varepsilon^p(x,t)). \tag{2}$$

The constitutive relations have the form of evolution equations

$$\dot{\boldsymbol{\varepsilon}}^p(x,t) = \Phi_{\varepsilon^p}(\boldsymbol{\sigma}(x,t), \boldsymbol{q}(x,t)), \qquad \dot{\boldsymbol{q}}(x,t) = \Phi_q(\boldsymbol{\sigma}(x,t), \boldsymbol{q}(x,t)) \qquad \forall x \in \Omega \tag{3}$$

with initial values $\boldsymbol{\varepsilon}^p(x,0) = \boldsymbol{\varepsilon}^p_0$, $\boldsymbol{q}(x,0) = \boldsymbol{q}_0$. Note that the internal state variables $\boldsymbol{q}$ can be either second order tensors or scalars.

The mathematical model outlined so far has been investigated by various authors. We refer here to Alber [1] where existence and uniqueness of solutions of the combined system (1) to (3) has been shown for a large class of constitutive equations. Furthermore, one could also view the combined system of balance and evolution equations as an example of a Partial Differential Algebraic Equation or PDAE, see [10] for first results in this field.

In the benchmark problem below, we consider the evolution equations of Chan-Bodner-Lindholm [3] under the assumption of homogeneous temperature. This approach belongs to the class of unified viscoplastic models due to Lubliner [9,2]. Our notation is similar to the notation used by Fritzen [5],

$$\begin{array}{rclcrcl}
\dot{\boldsymbol{\varepsilon}}^p & = & \varphi\, dev\, \boldsymbol{\sigma}/\|dev\, \boldsymbol{\sigma}\| & \qquad & \varphi & = & \sqrt{2}D_0 \exp\left[-\frac{1}{2}\left(\sqrt{\frac{2}{3}}\frac{Z}{\|dev\, \boldsymbol{\sigma}\|}\right)^{2n}\right] \\
\dot{Z}^{(i)} & = & m_1(Z_1 - Z^{(i)})w_p & & w_p & = & \boldsymbol{\sigma} : \dot{\boldsymbol{\varepsilon}}^p \\
\dot{\boldsymbol{\beta}} & = & m_2(Z_3 \cdot \boldsymbol{p} - \boldsymbol{\beta})w_p & & \boldsymbol{p} & = & \boldsymbol{\sigma}/\|\boldsymbol{\sigma}\|
\end{array}$$

with the scalar $Z = Z^{(i)} + \boldsymbol{\beta} : \boldsymbol{p}$ for isotropic hardening and the second order tensor $\boldsymbol{\beta}$ for directional hardening.

For simplicity, we concentrate now on the 2D case and assume plane stress. Let u still denote the displacement vector and introduce a vector notation for stress and strain and a Sobolev space V by [5]

$$\begin{array}{rcl}
\sigma & := & [\sigma_{11}, \sigma_{22}, \sqrt{2}\,\sigma_{12}]^T \\
L & := & \begin{bmatrix} \frac{\partial}{\partial x_1} & 0 \\ 0 & \frac{\partial}{\partial x_2} \\ \frac{\partial}{\sqrt{2}\partial x_2} & \frac{\partial}{\sqrt{2}\partial x_1} \end{bmatrix} \\
V & := & (H^1(\Omega))^2
\end{array}
\qquad
\begin{array}{rcl}
\varepsilon & := & [\varepsilon_{11}, \varepsilon_{22}, \sqrt{2}\,\varepsilon_{12}]^T = Lu(x,t) \\
D & := & \dfrac{E}{1-\nu^2}\begin{bmatrix} 1 & \nu & 0 \\ \nu & 1 & 0 \\ 0 & 0 & 1-\nu \end{bmatrix} \\
V_0 & := & \{w \in V : w|_{\partial\Omega_u} = 0\} \\
V_{\bar{u}} & := & \{w \in V : w|_{\partial\Omega_u} = \bar{u}\}
\end{array}$$

The weak form (principle of virtual work) of the equations of motion (1) then reads

$$0 = \int_\Omega [Lu(x,t) - \varepsilon^p(x,t)]^T\, DLv(x,t)\, dx - \int_\Omega f^T(x,t)v(x,t)\, dx - \int_{\partial\Omega_\sigma} \bar{t}^T(x,t)v(x,t)\, ds \tag{4}$$

for all $v \in V_0$, with solution $u \in V_{\bar{u}}$. Note that the plastic strain ε^p is still defined by the evolution equations (3) while the stress is expressed by the differential operator L and equation (2).

3. Discretization

As mentioned in Section 1, Finite Elements are the method of choice in viscoplasticity. For an analysis of space and time discretization techniques see, e.g., LeTallec[8]. In order to derive the discrete problem

$E[MPa]$	ν	D_0 [$\frac{1}{s}$]	n	Z_0 [MPa]	Z_1 [MPa]	Z_3 [MPa]	m_1 [$\frac{1}{\text{MPa}}$]	m_2 [$\frac{1}{\text{MPa}}$]
220000	0.298	9799	1.4753	378.2	868.4	332.5	0.2032	13.41

Table 1: Parameters for the model of Chan-Bodner-Lindholm, SS316 [11]

associated to (4), V_0 and $V_{\bar u}$ are replaced by finite dimensional subspaces $V_0^h \subset V_0$ and $V_{\bar u}^h \subset V_{\bar u}$ with basis functions $N_i, i = 1, \ldots, M$. With $\bar u^h \approx \bar u$ on $\partial\Omega_u$, we introduce the ansatz

$$u^h(x,t) = \sum_{j=1}^{M} N_j(x)u_j(t) + \bar u^h(x,t) =: N(x)u(t) + \bar u^h(x,t), \quad v^h(x,t) = \sum_{j=1}^{M} N_j(x)v_j(t) =: N(x)v(t).$$

Now, the discrete version of (4) can be formulated as

$$\begin{aligned} 0 \; = \; & \int_{\Omega^h} B^T(x)DB(x)u(t)\,dx - \int_{\Omega^h} B^T(x)D\varepsilon^p(x,t)\,dx \\ & - \int_{\Omega^h} N^T(x)f(x,t)\,dx - \int_{\partial\Omega^h_\sigma} N^T(x)\bar t(x,t)\,ds + \int_{\Omega^h} B^T(x)DL\bar u^h(x,t)\,dx \end{aligned} \tag{5}$$

with Ω and $\partial\Omega$ approximated by Ω^h, $\partial\Omega^h$ and $B(x) := [LN_1(x), \ldots, LN_M(x)]$.

Due to the plastic strain, the second integral in (5) has to be computed numerically. The application of a quadrature formula leads to

$$\int_{\Omega^h} B^T(x)D\varepsilon^p(x,t)\,dx \approx \sum_{k=1}^{\mu} \gamma_k B^T(\xi_k)D\varepsilon^p(\xi_k,t) =: C(\xi)\varepsilon^p(\xi,t)$$

with quadrature weights γ_k and quadrature points ξ_k. For the evaluation of $\varepsilon^p(\xi_k,t)$, the evolution equations (3) must be solved in every quadrature point.

Summing up, we obtain thus the semidiscretized equations

$$0 = Ku(t) - b(t) - C(\xi)\varepsilon^p(\xi,t) \qquad \text{and} \qquad \left.\begin{aligned} \sigma(\xi_k,t) &= D(B(\xi_k)u(t) - \varepsilon^p(\xi_k,t)) \\ \dot\varepsilon^p(\xi_k,t) &= \Phi_{\varepsilon^p}(\sigma(\xi_k,t), q(\xi_k,t)) \\ \dot q(\xi_k,t) &= \Phi_q(\sigma(\xi_k,t), q(\xi_k,t)) \end{aligned}\right\} \; k = 1,\ldots,\mu$$

where

$$\begin{aligned} K \; &:= \int_{\Omega^h} B^T(x)DB(x)\,dx \qquad\qquad \text{(stiffness matrix)} \\ b(t) \; &:= \int_{\Omega^h} N^T(x)f(x,t)\,dx + \int_{\partial\Omega^h_\sigma} N^T(x)\bar t(x,t)\,ds - \int_{\Omega^h} B^T(x)DL\bar u^h(x,t)\,dx \quad \text{(load vector).} \end{aligned}$$

Let $\hat\sigma, \hat\varepsilon^p$ and $\hat q$ denote vectors which comprise the components $\sigma(\xi_k,t), \varepsilon^p(\xi_k,t)$ and $q(\xi_k,t)$, $k = 1,\ldots,\mu$, respectively. If we define additionally differential variables $y := (\hat\varepsilon^p, \hat q)$ and algebraic variables $w := (u, \hat\sigma)$, the semidiscretized equations of motion can finally be written as Differential-Algebraic Equation (DAE)

$$\dot y(t) = f(y(t), w(t)), \qquad\qquad 0 = g(y(t), w(t)). \tag{6}$$

Standard DAE theory [6] shows that (6) is of index 1 iff the stiffness matrix K is invertible. The latter condition holds if enough supporting boundary conditions are specified. Consequently, DAE solvers can be applied to integrate (6) in time.

The most popular scheme is without doubt the implicit Euler since it meets several requirements:

	CPU-time	time steps	rejected steps	Newton failures	x-Error	y-Error	comments
Tensile test							
BDF2/1	34350	971	19	10	6.90e-08	1.10e-08	ATOL=RTOL=1e-3
BDF2/2	10722	300	20	1	2.84e-07	4.75e-08	ATOL as vector, RTOL=1e-3
Impl.Eul.	49372	1500	-	0	6.39e-07	9.98e-08	$\Delta t = 0.01$
Bended beam							
BDF2/1	77415	2372	22	8	4.96e-08	6.83e-07	ATOL=RTOL=1e-3
BDF2/2	15783	401	18	4	3.24e-07	4.49e-06	ATOL as vector, RTOL=1e-3
Impl.Eul.	49967	1500	-	0	1.63e-06	2.29e-05	$\Delta t = 0.01$

Table 2: Integration statistics for tensile and bended beam test with 8-node rectangular elements. The maximum displacement-error in x/y-direction was computed with respect to a BDF2 reference run and ATOL=RTOL=1e-6.

it is of order 1 in both y and w, it is A-stable, and it fits well in the FEM algorithms, which is very important in terms of implementation. However, stepsize control is also an important issue, and for this reason there is a growing interest in adapting DAE techniques to this particular problem class, see, e.g., [5].

For the benchmark problem below, we use an extension of the implicit Euler method which is, though of second order, almost as inexpensive to implement. The BDF-2 method for (6) with variable stepsize [6,7] reads

$$\begin{aligned} \frac{1+2\tau_n}{1+\tau_n} y_{n+1} - (1+\tau_n) y_n + \frac{\tau_n^2}{1+\tau_n} y_{n-1} &= h_n f(y_{n+1}, w_{n+1}) \\ 0 &= g(y_{n+1}, w_{n+1}). \end{aligned}$$

Here, y_{n+1} denotes the numerical solution of y at time $t = t_{n+1}$ with stepsize $h_n = t_{n+1} - t_n$ and stepsize ratio $\tau_n = h_n / h_{n-1}$. Note that the nonlinear system for y_{n+1} and w_{n+1} has the same dimension as in case of implicit Euler. For its solution, one can either apply a full or chord-Newton method or, by exploiting the strucure of the FEM grid, a two-stage Newton process [7]. The latter technique solves first the discretized evolution equation in each element and then computes a global iterate from the discretized balance equations.

The stepsize control relies on a predictor-corrector scheme as local error estimator. With absolute and relative tolerances ATOL and RTOL, the stepsize is selected such that the local error estimation Δz, $z = (y, w)$, satisfies $\|\Delta z\| \leq 1$ in a standard weighted root mean square norm [6]

$$\|\Delta z\|^2 := \frac{1}{l} \sum_{i=1}^{l} \left(\frac{\Delta z^i}{\mathrm{RTOL} \cdot \mathrm{WT}^i + \mathrm{ATOL}^i} \right)^2 \quad \text{for } \Delta z = (\Delta z^1, \ldots, \Delta z^l)\,. \tag{7}$$

The weight vector WT is defined by some reference data, e.g., $\mathrm{WT} = z_{n+1}$ which is the new solution at time t_{n+1}.

4. Benchmark problem

The following example is chosen as a benchmark problem since it is often used in experimental identification and since typical viscoplastic effects can be observed. A beam of length 1m and height 0.2m is subjected to a tensile test, Fig. 1. First, the loading increases linearly, then the beam is held fixed,

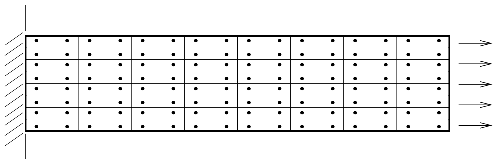

Figure 1: Tensile test of a viscoplastic beam

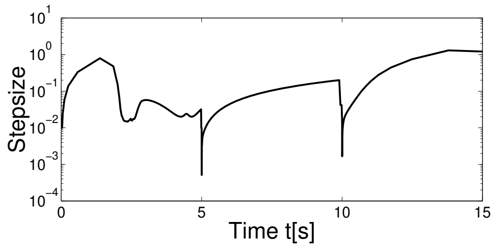

Figure 2: Stepsize control

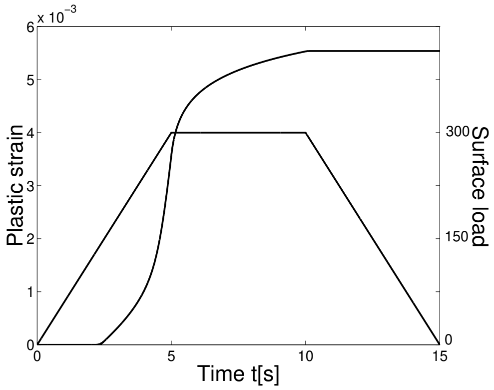

Figure 3: Plastic strain ε_{11}^p and loading

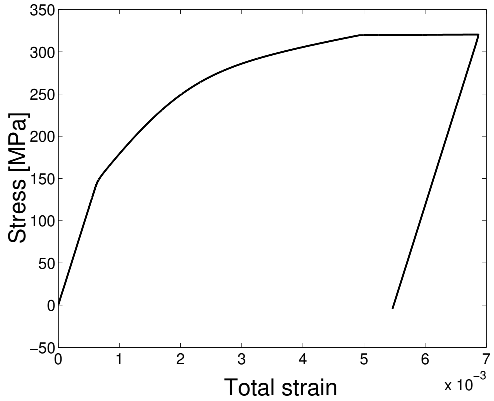

Figure 4: Stress-strain-diagram (σ_{11}, ε_{11})

and finally the loading decreases again linearly to zero, see Fig. 3. Each phase takes 5 seconds. We use the unified viscoplastic model of [3] for the stainless steel SS316 (nickel-chromium, single crystal). The parameters given in Table 1 were identified by Seibert [11].

Assuming plane stress, the beam is discretized by 32 8-node rectangular finite elements, and second order Gaussian quadrature is used in each element. Thus, the DAE (6) obtained from space discretization features 896 differential variables y and 1010 algebraic variables w. For time integration, both implicit Euler and BDF-2 were employed. Fig. 3 shows the plastic strain ε_{11}^p and Fig. 4 the stress-strain diagram for σ_{11} and ε_{11} in the upper left corner of the beam.

As demonstrated by Fig. 2, the BDF-2 stepsize increases in regions with purely elastic behavior and in the holding phase whereas it decreases when plastic deformations occur and also at points of phase transition. In particular, at time $t = 5$s and $t = 10$s, the change in the loading is reflected by sharp stepsize drops since such discontinuities were not taken into account by root finding techniques. Table 2 compares BDF-2 with implicit Euler. Both methods solve here in each step the system of nonlinear equations by a chord-Newton process. In order to stabilize and speed up these computations, we supplied an analytical Jacobian evaluation and used sparse matrix techniques. Clearly, the BDF-2 scheme is more accurate and much faster than implicit Euler. Due to the different scales of variables that range from $1e-3$ for plastic strains to $1e+2$ for stresses, the stepsize control can be significantly improved by choosing ATOL as vector (BDF2/2), compare (7). The BDF-2 method takes then only 20% of the computing time of implicit Euler while still delivering a more accurate result.

The above results are confirmed by a second example where the beam is subjected to a bending test, Fig. 5. Corresponding simulation results are shown in Figures 6 to 8. It turns out that, due to a higher strain and stress growth, the number of time steps increases here, especially in the loading phase.

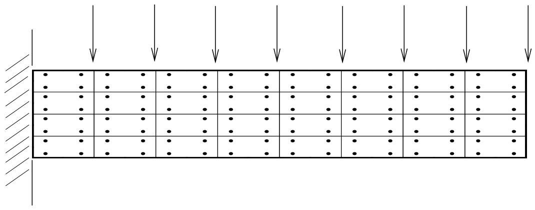

Figure 5: Bending test of a viscoplastic beam

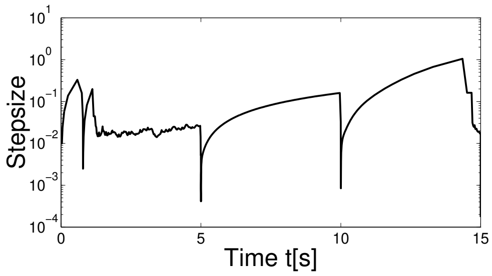

Figure 6: Stepsize control

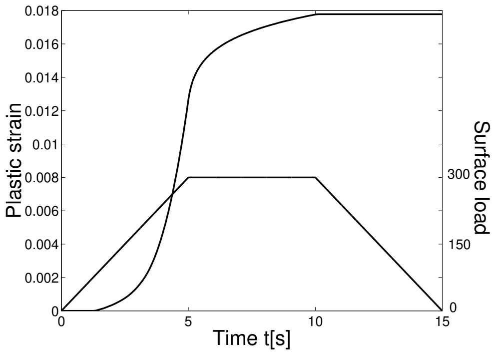

Figure 7: Plastic strain ε_{11}^p and loading

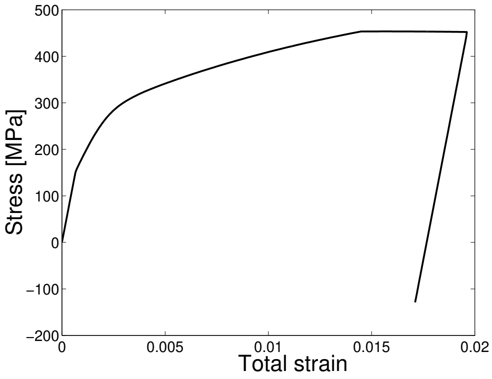

Figure 8: Stress-strain-diagram $(\sigma_{11}, \varepsilon_{11})$

Nevertheless, the stepsize control leads again to a much more efficient simulation. Choosing ATOL as vector to account for different ranges of variables works even better than before.

To summarize, the benchmark problem shows that DAE solvers such as the BDF-2 method can improve both accuracy and efficiency in viscoplastic simulation. However, there are further aspects which should be considered as well in the future, in particular the interplay of space and time discretization and the loading vector $b(t)$. The latter is the driving force of the process and supplies valuable additional information.

Acknowledgements

The authors would like to thank P. Rentrop and W.C. Rheinboldt for many helpful discussions. This research is supported by the DFG within SFB298 'Deformation und Versagen bei metallischen und granularen Strukturen'.

5. References

1 Alber, H.D.: Initial-Boundary Value Problems for the Inelastic Material Behavior of Metals. Springer Lecture Notes in Mathematics 1682 (1998).

2 Bodner, S.R.: Review of a Unified Elastic-Viscoplastic Theory. In Miller,A. (ed): Unified Constitutive Equations for Plastic Deformation and Creep. Elsevier Applied Science, London (1987) 273-301 .

3 Chan,K.S.;Bodner,S.R.;Lindholm,U.S.: Phenomenological Modeling of Hardening and Thermal Recovery in Metals. Journal of Engineering Materials and Technology Vol.110, 1-8 (1988).

4 Cordts,D.;Kollmann,F.G.: An implicit time integration scheme for inelastic constitutive equations with internal state variables, Int.J.Num.Meth.Eng.,Vol.23, 533-554 (1986).

5 Fritzen,P.: Numerische Behandlung nichtlinearer Probleme der Elastizitäts- und Plastizitätstheorie. PhD.-thesis, Technische Hochschule Darmstadt (1997).

6 Hairer,E.;Wanner,G.: Solving Ordinary Differential Equations II. 2nd Ed., Springer-Verlag, (1996).

7 Kirchner,E.;Simeon,B.: A higher order time integration method for viscoplasticity, submitted for publication in Comp. Meth. Appl. Mech. Engng. (1997).

8 LeTallec,P.: Numerical Methods for Nonlinear Elasticity. In: Ciarlet, P., Lions, J.(eds.): Handbook of Numerical Analysis III. North-Holland (1994).

9 Lubliner,L.: Plasticity Theory. Macmillan Publishing Company (1990).

10 Lucht,W.;Strehmel,K.;Eichler-Liebenow,C.: Linear Partial Differential Algebraic Equations Part I: Indexes, Consistent Boundary/Initial Conditions, Report U. Halle-Wittenberg (1997).

11 Seibert,T.: Simulationstechniken zur Untersuchung der Streuung bei der Identifikation der Parameter inelastischer Werkstoffmodelle. PhD.-thesis, Technische Hochschule Darmstadt (1996).

12 Wriggers,P.;Eberlein,R.;Reese,S.: A comparison of three-dimensional continuum and shell elements for finite plasticity, International Journal of Solids and Structures, Vol. 33, 3309-3326 (1996).

Addresses: Dipl.Math. Oliver Scherf, Dr. Bernd Simeon Technische Universität Darmstadt, Fachbereich Mathematik, AG Wissenschaftliches Rechnen, Schloßgartenstr. 7, 64289 Darmstadt, Germany.

e-mail: scherf@mathematik.tu-darmstadt.de or simeon@mathematik.tu-darmstadt.de